Sol-Gel Processes in Micro-Environments of Black Shale: Learning from the Industrial Production of Nanometer-Sized TiO₂ Polymorphs

Hans-Martin Schulz

Helmholtz Centre Potsdam GFZ—German Research Centre for Geosciences, Section 3.2 Organic Geochemistry, D-14473 Potsdam, Germany; schulzhm@gfz-potsdam.de; Tel.: +49-331-288-1789

check for updates

Abstract: Micro-environments in black shale are reactors for geochemical reactions that differ from the bulk scale. They occur in small isolated pores of several 10 s to 100 s of nanometers without or with limited ionic exchange by diffusion to the surrounding matrix. The example of the formation of titania polymorphs brookite (and anatase) in black shale demonstrates that pH < 4 of the pore waters or lower must prevail to enable dissolution of Ti-bearing precursors followed by the precipitation of these metastable solids. Comparably low pH is applied during the industrial production of nanometer-sized brookite or anatase by sol-gel methods. The process parameters during industrial production such as low pH, negative Eh, or low ionic strength (to promote agglomeration) allow a comparison with parameters during geochemical processes leading to titania formation in black shale. Sol-gel processes are suggested herein as key geochemical processes in micro-environments of black shale in order to understand the formation of single brookite crystals or agglomerates on a nanometer scale.

Keywords: black shale; brookite; micro-environment; sol-gel process

---

1. Introduction

Shale is a fine-grained, siliciclastic sediment with high water content. Porosity-depth trends indicate a loss in porosity (and thus in water content) from initially up to 80% to less than 20% at a depth of around 3000 m, dependent on burial history and composition [1]. Porosity in shale comprises of a variety of pores which occur in the organic material as well as in or between minerals [2,3]. These pores range in size from macropores (diameter > 50 nm), to mesopores (2–50 nm), to micropores (<2 nm; [4]) and have been described in great detail in shale research as an unconventional resource [5,6]. Pores of small size especially are considered spots for geochemical reactions that are different from the bulk scale and may act as isolated micro-environments for the localized dissolution and precipitation of solids. Much of the porosity can be filled with formation water (besides liquid and gaseous hydrocarbons). This aqueous phase is a matrix, reactant, and transport medium during rock–fluid interactions at various scales [7–9].

In this contribution, a characteristically exemplary micro-environment for the formation of nanometer-sized titania polymorphs in black shale is introduced—its significance for localized organic–inorganic interactions apart from the bulk scale. By explaining the formation of nano-sized titanium dioxide in black shale, reference is made to today´s technical sol-gel processes for the production of titania nanomaterials at low temperatures under controlled physicochemical conditions. Several experimental parameters are compared with those under geological subsurface conditions to find similar controls on the formation, fate, and behavior of brookite (and anatase) in organic-rich sediments and comparable processes in other organic-rich and aqueous environments, such as oil–water contacts in oil fields.

The selected example relates to the metastable titania (TiO_2) polymorphs brookite and anatase, and how they form in black shale environments [10]. This issue is reconsidered in this short communication, but with reference to the prenucleation concept and the so-called sol-gel process. Selected titania polymorphs (only brookite in this research) in black shales will be presented in the form of an image collection highlighting micro-environments on a micrometer to nanometer scale, and their formation will be discussed as controls of organic matter conversion in micro-environments as analogues of industrial nano-titania production.

2. Geochemical Micro-Environments in General and in Black Shale—A Brief Review

Chemical microenvironments are well-known phenomena in various geological matrixes and are reported from shale [11–13], hardgrounds [14], soils [15,16], and fluvial systems [17], but also occur in sediment macrofauna [18], living planktic foraminifera [19], or in fecal pellets [20]. One often reported feature is the formation of iron-bearing solid solutions in various geological matrixes such as marine sediments [21], glaciers [22], or even on Mars [23], but many other minerals also dissolve or precipitate in such microenvironments which suggest geochemical processes different from those of the bulk matrix.

A geochemical micro-environment in a rock can be defined as a small entity within a bulk rock matrix. It is filled by a fluid with a composition that is different from the bulk composition. Such a fluid can be physically isolated from the bulk solution or not. A definition by Reference [24] also includes scale considerations from a large scale (e.g., clay lenses in sandy sediments) to nanometer scale. The authors stated that micro-environments can be found at mineral interfaces or contacts [25], within mineral grains [26], or even at the microbial cell surface on the sub-micron to micron scale. At the nanometer scale, a microenvironment may involve different reacting molecular sites represented by the reactivities of different mineral surface faces or at their intersections. Recently it was found that micro-environments also play a significant role in preserving organic fossils due to interactions between clay minerals and organic tissues. Conversion or decay of organic matter may be inhibited by blocked enzymatic reactions [27].

The processes leading to the development of microenvironments in shale are dependent on chemical gradients which develop in the aqueous phase due to fast reaction rates (either microbially mediated or mineral dissolution/precipitation rates) and compensate the export or import of solutes [24]. Due to this definition, preferential sites for the development of micro-environments are physically heterogeneous systems with different flow rates and molecular diffusion as the main transport processes. Accordingly, micro-environments can be retraced by the occurrence of features such as concretions in shale of various scales.

Characteristic hydrogeochemical conditions develop due to organic–inorganic interactions in chemical micro-environments of black shales. The driving force for the creation of localized hydrogeochemical conditions in such micro-environments (or microreactors) is the conversion of labile organic matter (OM). The OM consumption already takes place in the overlying water column where microreactors may form in sinking particles, such as in anoxic bottom water (e.g., pyrite framboid formation; [2]). Later, they develop during deposition and continue from early diagenesis to the oil window and beyond, all dependent on the sensitivity of the preserved but still reactive to organic matter. The processes in micro-environments are thus not affected by the buffer potential of the bulk rock. However, during subsidence in a sedimentary basin, a variety of soluble organic compounds are released from the organic material which control different hydrogeochemical processes—as these compounds may change in pH. For example, during early diagenesis to the oil window, acidic and corrosive hydrogeochemical conditions develop due to the release of low molecular weight organic acids (e.g., acetic acid) or carbon dioxide and lead to dissolution of unstable minerals, which is compensated by the precipitation of solid solutions at equilibrium [28].

3. Formation of Inorganic Materials from Solutions

Stawski and Benning [29] reviewed how amorphous and crystalline inorganic materials may form from solutions. In summary, precipitation and growth of any solid material from a solution are dynamic processes during which different species of various shapes, sizes, and internal structures form and further develop into a final product. In this paper, two hypotheses are discussed for the explanation of nucleation and crystallization phenomena taking place in solutions—the classical nucleation theory (CNT) and the prenucleation concept (see references in [29]). Although different in their individual process chains, the conceptual pathways described for both approaches consider the formation of nanostructures from a solution to a stable end-product. A well-balanced interplay of the physical and chemical parameters controls the morphology and growth kinetics of these nanostructures in evolving systems. It is important to note that the prenucleation concept also refers to intermediate stages of amorphous particles (Figure 1A). In a sol-gel process, a sol (colloidal suspension) is formed from the hydrolysis and polymerization reactions of the precursors, which are inorganic metal salts or metal organic compounds such as metal alkoxides (Figure 1B). The transition from the liquid sol into a solid gel phase is caused by complete polymerization and loss of the solvent [30].
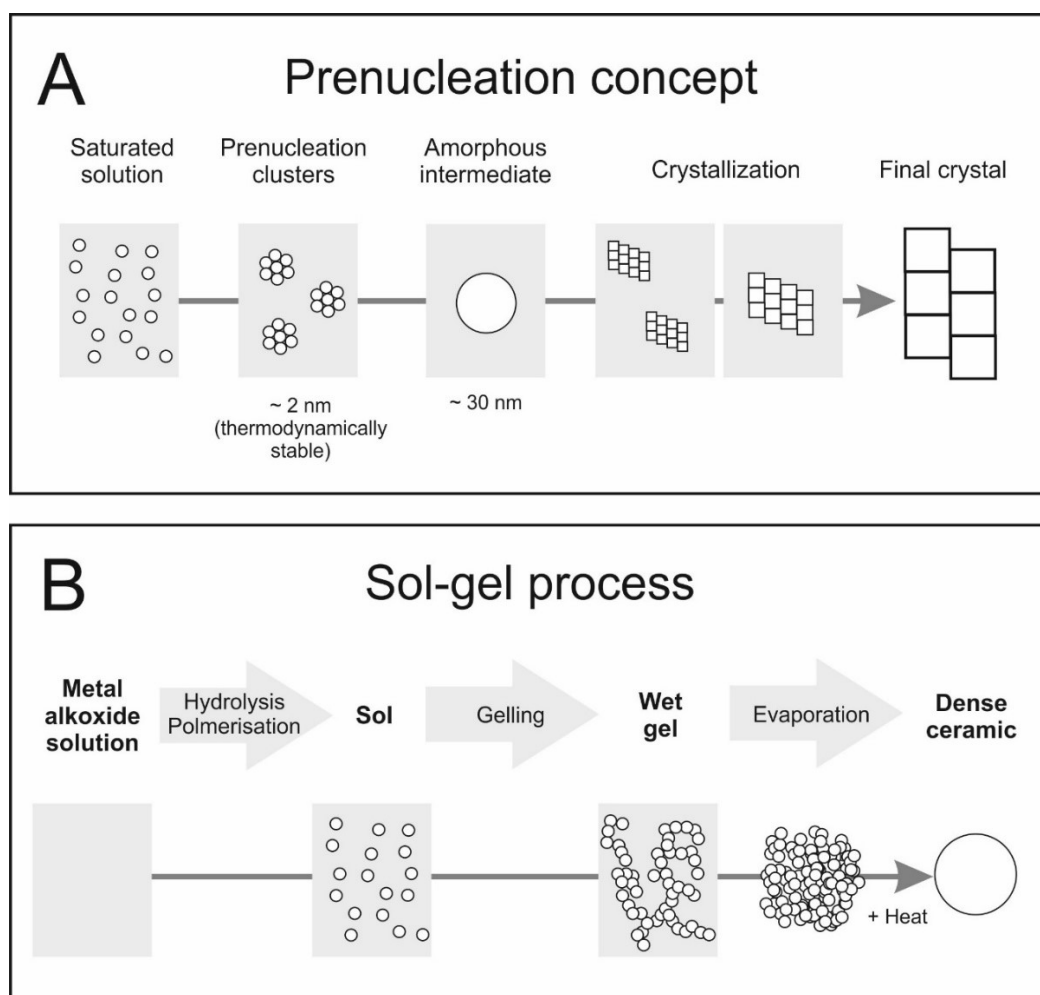

Figure 1. (**A**) Nonclassical pathway for the growth of crystalline materials from solutions. (**B**) Scheme representing the evolution of aqueous silica system from monomers to developed sols and gels, in relation to reaction conditions. (**A**) is redrawn after Figure 5.2 in Reference [29]; see details for references therein. (**B**) Various steps in the sol-gel process to control the final morphology of the product (redrawn after Figure 2.1. in Reference [30]).

4. Methodologies to Characterize and Analyze Micro-Environments

The analysis of micro-environments requires chemical or imaging techniques that are capable of characterizing small volumes or small sizes. However, their applicability can be limited by the close association with the bulk phases. Moreover, the geochemical modelling of micro-environments in shale by PHREEQC—a program based on chemical thermodynamics—may be problematic due to the low pH in micro-environments and due to migration of acidic capillary pore water [31], but general approaches have existed since the 1970s [32].

The analytical approach used here was based on a first overview characterization of the black shale by conventional light microscopy. In a second step, scanning electron microscopy (SEM) with a coupled energy dispersive X-ray spectroscopy (EDS) enabled the analysis of different shale entities. Contents of organic carbon (total organic carbon, TOC) were determined and Rock Eval analyses of whole rock samples were carried out according to standard procedures to characterize the amount, character, and maturity of the organic material. The final and main technique applied for visualization and characterization of micro-environments was transmission electron microscopy (TEM). Selected results from TEM investigations are presented, and brookite identification is based on the method described in Reference [10]. Samples for TEM investigations were prepared applying the focused ion beam (FIB) technique (detailed in Reference [33]).

5. Example Brookite (and Anatase): Formation of Unstable Titania Polymorphs in Micro-Environments of Black Shale

The titania polymorph brookite (Figures 2 and 3) mainly occur as a single crystal—less as agglomerated nano-crystals—in organic matter-rich sediments of differing age and thermal maturity [10], and single brookite crystals increase in diameter with increasing thermal maturity. In contrast, anatase prevails as both single crystals or as agglomerates at oil–water contacts in oilfields, and along fractures with fluid flow enriched in dissolved organic carbon. In general, titania nano-crystal precipitation, growth (and agglomeration) takes place in the pore water of micro-environments at low to high temperatures, and where low pH is coupled to the occurrence of dissolved organic components. Low sedimentation rates preserving a critical geochemical environment or higher temperatures seem to be major controls for the precipitation of anatase (cf. Figure 4) and its tendency not to agglomerate.
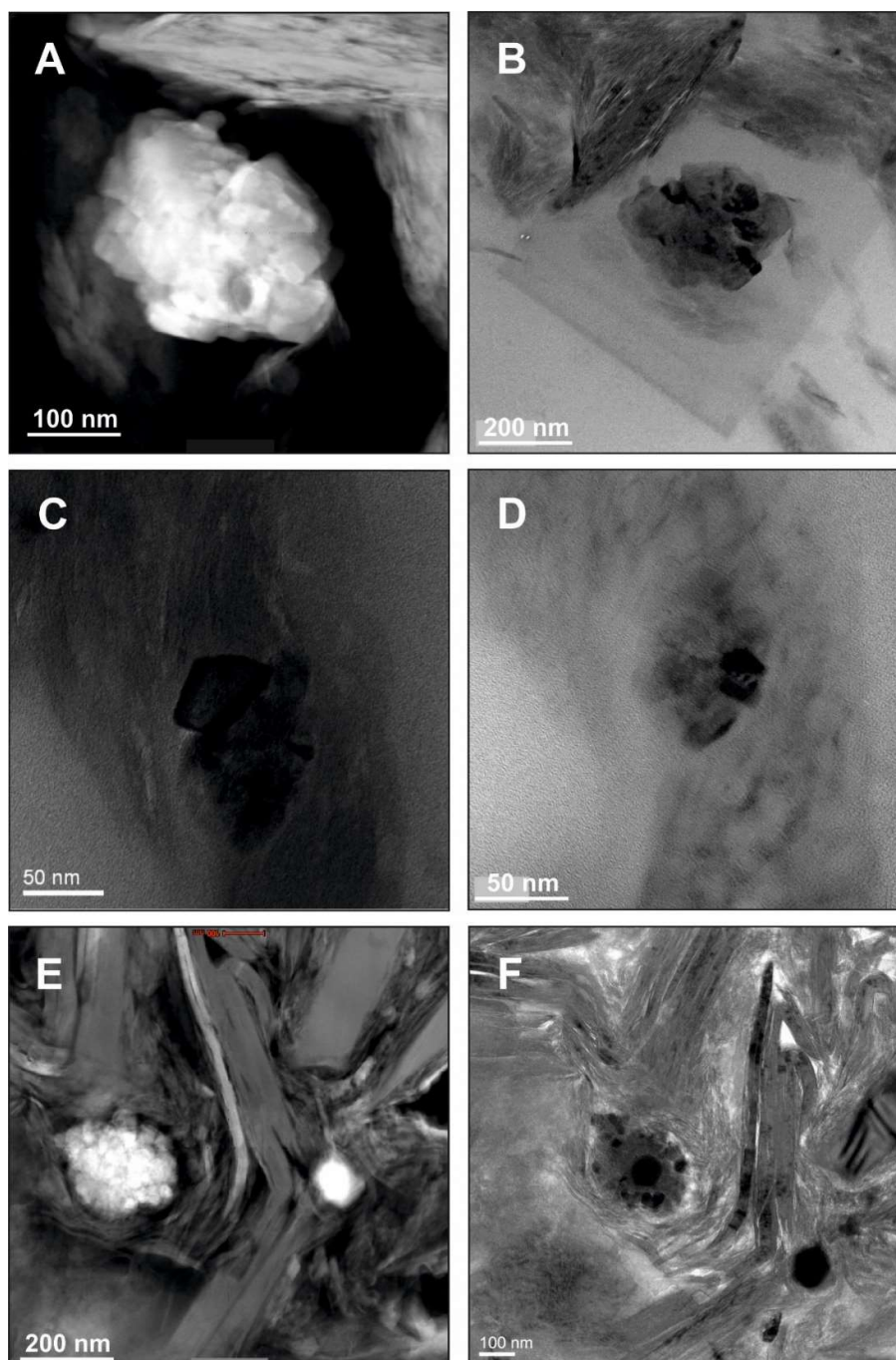
Figure 2. Titania (TiO$_2$) polymorphs (brookite in all selected samples) in selected black shales: Bakken Shale (**A,B**), Mediterranean sapropel S6 (**C,D**), and Schöneck Formation (**E,F**). (**A,C,D**) are high-magnification scanning transmission electron microscopy (STEM) images (high-angle annular dark-field (HAADF) mode), whereas (**B,D,F**) are TEM Bright Field images. The Pleistocene Mediterranean Sapropel S6 from the Eastern Mediterranean Sea was recovered from a sediment depth of 4.12 m (water depth, 2788 m), has a total organic carbon (TOC) content of 4–6%, and is composed of marine organic matter (OM). The sample from the Oligocene Schöneck Fm. (Upper Austrian Molasse basin) originates from a well core from a depth of 1384 m, has a TOC content of 3.6%, and an immature lacustrine OM (hydrogen index, HI: 550 mg HC/g TOC). The Bakken Shale sample is of Upper Devonian to Lower Mississippian age, was drilled in the Williston Basin (North Dakota, U.S.A.), and comes from a depth of 2332 m. The TOC content is 8.3%, the marine OM has a HI of 416 mg HC/g TOC and an oxygen index (OI) of 27 mg CO$_2$/g TOC.
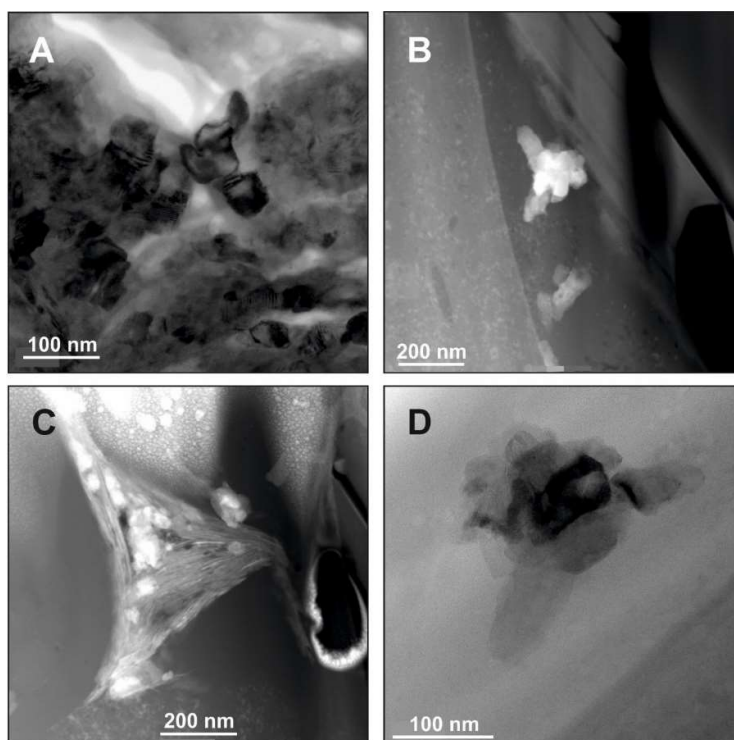
Figure 3. Titania (TiO$_2$) polymorphs (brookite in all selected samples) in the Dictyonema Shale (Tremadocian, Ordovician). (**A**,**D**) are TEM Bright Field images whereas (**B**,**C**) are high-magnification scanning transmission electron microscopy (STEM) images (high-angle annular dark-field (HAADF) mode). (**A**) The sample originates from a well core from a depth of 52.05 m, has a TOC content of 12.20%, and is early mature (hydrogen index, HI: 191 mg HC/g TOC; T$_{max}$: 414 °C). (**B**,**C**,**D**) The sample originates from a well core from a depth of 52.40 m, has a TOC content of 6.15%, and is early mature (hydrogen index, HI: 95 mg HC/g TOC; T$_{max}$: 414 °C).
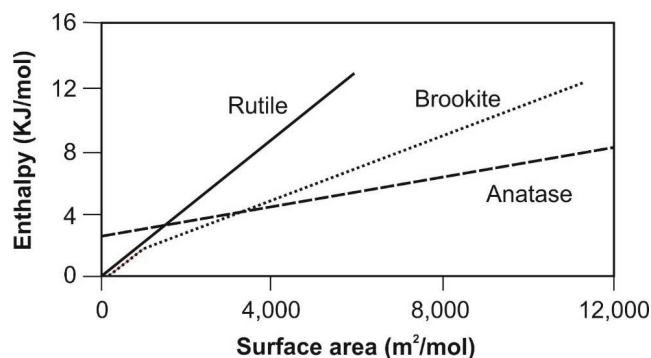

Figure 4. Enthalpy of titania polymorphs as a function of surface area (already presented in Reference [10], redrawn after Reference [34], following Reference [35]). Although the crystalline polymorph rutile is thermodynamically the most stable one, anatase and brookite are often slightly metastable by only a few kilojoules per mole. Brookite has a surface enthalpy of approximately 1.0 J/m^2, which is higher than for anatase (0.4 J/m^2). Moreover, for titania particles with a surface area higher than around 4000 m^2/mol (thus for smallest particles), anatase has the lowest enthalpy and can directly transform into brookite [35]. At a crossover size of about 30 nm, anatase nanoparticles may directly transform into rutile [34,36].

6. Industrial Production of Titania Polymorphs

Low temperature industrial processes may serve as process analogues to extract relevant key variables which might also control hydrogeochemical processes during diagenesis of black shales.

However, sedimentary geosystems are complex and variable in time and space. The geochemical composition of the interacting organic–inorganic rock–fluid–gas inventory in sedimentary geosystems thus changes with geological times. Moreover, the material properties of industrial TiO_2 nanoparticles strongly depend on the detailed production methodology and lead to different nanoparticle sizes, crystal structures, and morphologies. Thus, the variety of experimental conditions used for the artificial synthesis of the different TiO_2 phases complicate a direct comparison with natural mechanisms during nanoparticle formation in a black shale. As a logical consequence, a direct transfer of factors, phenomena, and their controls in laboratory experiments under controlled conditions to the geosphere must be critically scrutinized. Nevertheless, there are basic physicochemical factors that resemble in black shales during laboratory experiments and during sol-gel processes for the industrial production of nanotitania.

Today, the most widely used industrial process for the production of metal oxides is the ceramic method, which is based on high temperature treatment (several 100s of °C) of powder mixtures and results in thermodynamically stable phases rather than brookite [30]. However, comparably low temperatures down to ~80 °C prevail in TOC-rich fine-grained sediments until a depth of around 2 km (considering a general geothermal gradient with a mean surface temperature of 20 °C). According to this, the sol-gel process is chosen as the industrial analogue for comparison (details in overview articles such as References [37,38]). In general, aqueous and non-aqueous sol-gel chemical methods must be differentiated Reference [39]. Non-aqueous sol-gel processes are performed in organic solvents. In contrast, the aqueous alternative is described as the polymerization reaction of a dissolved metal chloride, nitrate, or sulfate (also of an organic compound, [30]). Hence, for the purpose of this short contribution, reference is made to the aqueous method as a comparative analogue for hydrogeochemical processes in sedimentary basins.

There are several physical and chemical parameters in aqueous sol-gel experiments that are key variables for the formation of brookite (and anatase). Such parameters may thus also control their formation and aggregation in black shales and resemble in (i) pH, (ii) ionic strength, and (iii) addition of acetic acid (and others, e.g. oxalic acid, fulvic/humic acid, etc).

The pH of the aqueous solution is a major control for brookite formation in sol-gel processes. Pottier et al. [40] showed that brookite exclusively forms from a strongly acidic aqueous 0.05 mol/dm^3 $TiCl_4$ solution at 100 °C, and that higher $TiCl_4$ concentrations favor rutile precipitation. Brookite is thus the major phase experimentally obtained in the range $17 \leq Cl:Ti \geq 35$ with 0.15 mol dm^3 Ti. The Cl:Ti molar ratio thus controls the kind of generated crystalline phases and their relative proportions, but also the particle size. Moreover, a suitable ratio also avoids recrystallisation of brookite into rutile during ageing in suspension. As a result of these investigations, the complex $Ti(OH)_2(Cl)_2(OH_2)_2$ is suggested to be the precursor of the brookite phase and dissolved chloride ions stabilize brookite in suspension. Li et al. [41] also demonstrated a phase-selective synthesis of titania nanocrystals at 180 °C (3 h) at pH lower than 2 and observed that nano-brookite was formed by a controlled coupling of pH and $TiCl_3$ concentrations. In general, anatase formed at high pH. Bhave and Lee [42] synthesized nanocrystalline brookite particles at pH 2 using dissolved $TiCl_4$ with isopropanol as the co-solvent in hydrochloric acid. The resultant gel mass was peptized and crystallized under refluxing condition for 15 h at 83 °C to a pure brookite phase. However, brookite also formed at 70 °C and 100 °C, but often together with rutile and/or anatase. The addition of hydroxypropyl cellulose yielded a more uniform particle size along with decreasing agglomeration tendencies. This addition of organic compounds plays a further key role in the precipitation of TiO_2 nanocrystals via aqueous sol-gel syntheses. For example, adsorption of humic acids and zeta potential are known to be dependent on pH and thus control aggregation. At low pH the amount of adsorbed humic or fulvic acids is high and thus lowers aggregation [43,44]. Moreover, synthesis by the sol-gel route using ethylene glycol as a gelling agent results in 19 nm-sized anatase [45]. Other organic gelation agents are ammonia [46] or citric acid and acetyl acetone as complex agents [47]. However, there is a variety of organic compounds used as solvents, surfactants, or additives in sol-gel methods to synthesize titania particles [48].

In a series of papers about sol-gel synthesis of titania nanoparticles by Isley and Penn [49,50] and Isley et al. [51,52], the effects of pH and ionic strength on the growth of brookite and anatase, as well as their contents and particle sizes were studied. In general, anatase is the primary product of such sol-gel syntheses at pH lower than 0. Brookite content and particle sizes can be controlled by varying the pH of the sol-gel synthesis.

Sol-gel methodological experiments under controlled aqueous conditions at room temperature showed that titanium dioxide primary particles of 4–5 nm in size readily form stable aggregates with an average diameter of 50–60 nm at pH ~4.5 in a NaCl suspension adjusted to an ionic strength of 0.0045 M [53]. A rapid formation of micron-sized aggregates occurs by solely increasing ionic strength to 0.0165 M, but also at pH values up to 8.2. Similar results may be achieved by applying $CaCl_2$ suspensions and indicate that divalent cations may enhance aggregation of nano-TiO_2 in soils and surface waters.

In summary, the findings of industrial processes, mainly over the sol-gel route, provide general insights into controls of nano-brookite formation under controlled conditions in the laboratory. Natural processes are more complex and change in time and space, but general findings may serve to better understand brookite formation in black shale.

7. Conclusions and Outlook

Hydrogeochemical processes in micro-environments of black shale can completely differ from processes of the bulk rock. The controlling factors and reasons for this difference is locally lacking permeability. This situation leads to geochemical processes in semi-closed systems as spots with localized and differing hydrogeochemical conditions.

The formation of nano-sized titania polymorphs serves as one example for processes in micro-environments and suggests that sol-gel processes take place in black shale. However, similar processes may occur whenever comparable conditions are caused by the co-occurrence of water, dissolved carbon dioxide or acetic acid, and solid phases with low stability against pH changes of the pore water. The dissolution of carbon dioxide and acetic acid in pore water leads to lower pH and, in the following, to the dissolution of matrix solids. However, a mandatory prerequisite is an isolated space, small or large, to keep pH low.

There is a broad spectrum of sedimentary environments in which similar factors may control sol-gel processes in isolated micro-environments, e.g. oil–water contacts in oil fields [10], or during barite precipitation at the sulphate–methane transition zone (SMT; [54]). However, the controlling factors may also prevail in non-sedimentary environments, e.g. in volcanic or seismically active areas [55], where aqueous fluids are in contact with organics.

Conflicts of Interest: The authors declare no conflict of interest.

References

1. Mondol, N.H.; Bjørlykke, K.; Jahren, J.; Høeg, K. Experimental mechanical compaction of clay mineral aggregates—Changes in physical properties of mudstones during burial. *Mar. Petrol. Geol.* **2007**, *24*, 289–311. [CrossRef]
2. Ross, D.A.; Degens, E.T. Recent sediments of the Black Sea. In *Black Sea-Geology, Chemistry, and Biology*; Degens, E.T., Ross, D.A., Eds.; American Association of Petroleum Geologist Memoir: Tulsa, Ok, USA, 1974; Volume 20, pp. 183–199.
3. Slatt, R.M.; O'Brien, N.R. Pore types in the Barnett and Woodford gas shales: Contribution to understanding gas storage and migration pathways in fine-grained rocks. *AAPG Bull.* **2011**, *95*, 2017–2030. [CrossRef]

4.   Sing, K.S.W.; Everett, D.H.; Haul, R.A.W.; Moscou, L.; Pierotti, R.A.; Rouquerol, J.; Siemieniewska, T. Reporting physisorption data for gas/solid systems with special reference to the determination of surface area and porosity (Recommendations 1984). *Pure Appl. Chem.* **1985**, *57*, 603–619. [CrossRef]

5.   Bernard, S.; Horsfield, B.; Schulz, H.-M.; Wirth, R.; Schreiber, A.; Sherwood, N. Geochemical evolution of organic-rich shales with increasing maturity: A STXM and TEM study of the Posidonia Shale (Lower Toarcian, northern Germany). *Mar. Petrol. Geol.* **2012**, *31*, 70–89. [CrossRef]

6.   Bernard, S.; Wirth, R.; Schreiber, A.; Schulz, H.-M.; Horsfield, B. Formation of nanoporous pyrobitumen residues during maturation of the Barnett Shale (Fort Worth Basin). *Int. J. Coal Geol.* **2012**, *103*, 3–11. [CrossRef]

7.   Van Berk, W.; Schulz, H.-M.; Fu, Y. Controls on CO2 fate and behavior in the Gullfaks oilfield (Norway): How hydrogeochemical modeling can help to decipher organic–inorganic interactions. *AAPG Bull.* **2013**, *97*, 2233–2255. [CrossRef]

8.   Fu, Y.; van Berk, W.; Schulz, H.-M.; Mu, N. Berthierine formation in reservoir rocks from the Siri oilfield (Danish North Sea) as result of fluid-rock interactions: Part II. Deciphering organic–inorganic processes by hydrogeochemical modeling. *Mar. Petrol. Geol.* **2015**, *65*, 317–326. [CrossRef]

9.   Schulz, H.-M.; Biermann, S.; van Berk, W.; Krüger, M.; Straaten, N.; Bechtel, A.; Wirth, R.; Lüders, V.; Schovsbo, N.H.; Crabtree, S. From shale oil to biogenic shale gas: Retracing organic–inorganic interactions in the Alum Shale (Furongian–Lower Ordovician) in southern Sweden. *AAPG Bull.* **2015**, *99*, 927–956. [CrossRef]

10. Schulz, H.-M.; Wirth, R.; Schreiber, A. Nano-crystal formation of TiO2 polymorphs brookite and anatase due to organic–inorganic rock-fluid interactions. *J. Sediment. Res.* **2016**, *86*, 59–72. [CrossRef]

11. Ruiz Cruz, M.D.; Reyes, E. Kaolinite and dickite formation during shale diagenesis: Isotopic data. *Appl. Geochem.* **1998**, *13*, 95–104. [CrossRef]

12. Cockell, C.S.; Pybus, D.; Olsson-Francis, K.; Kelly, L.; Petley, D.; Rosser, N.; Howard, K.; Mosselmans, F. Molecular Characterization and Geological Microenvironment of a Microbial Community Inhabiting Weathered Receding Shale Cliffs. *Microb. Ecol.* **2011**, *61*, 166–181. [CrossRef] [PubMed]

13. Schieber, J. *Iron Sulfide Formation. Encyclopedia of Geobiology*; Reitner, J., Thiel, V., Eds.; Springer: Amsterdam, The Netherlands, 2011; pp. 486–502.

14. Wilson, M.A.; Palmer, T.J.; Guensburg, T.E.; Finton, C.D.; Kaufman, L.E. The development of an Early Ordovician hardground community in response to rapid sea-floor calcite precipitation. *Lethaia* **1992**, *25*, 19–34. [CrossRef]

15. Ellis, A.G.; Weis, A.E. Coexistence and differentiation of 'flowering stones': The role of local adaptation to soil microenvironment. *J. Ecol.* **2006**, *94*, 322–335. [CrossRef]

16. Jiang, N.; Cai, D.; He, L.; Zhong, N.; Wen, H.; Zhang, X.; Wu, Z. A Facile Approach to Remediate the Microenvironment of Saline–Alkali Soil. *ACS Sustain. Chem. Eng.* **2015**, *3*, 374–380. [CrossRef]

17. Sánchez-Román, M.; Fernández-Remolar, D.; Amils, R.; Sánchez-Navas, A.; Schmid, T.; San Martin-Uriz, P.; Rodríguez, N.; McKenzie, J.A.; Vasconcelos, C. Microbial mediated formation of Fe-carbonate minerals under extreme acidic conditions. *Sci. Rep.* **2014**, *4*. [CrossRef]

18. Stief, P.; de Beer, D. Probing the microenvironment of freshwater sediment macrofauna: Implications of deposit-feeding and bioirrigation for nitrogen cycling. *Limnol. Oceanogr.* **2006**, *51*, 2538–2548. [CrossRef]

19. Wolf-Gladrow, D.A.; Bijma, J.; Zeebe, R.E. Model simulation of the carbonate chemistry in the microenvironment of symbiont bearing foraminifera. *Mar. Chem.* **1999**, *64*, 181–198. [CrossRef]

20. Bennett, R.H.; Bryant, W.R.; Hulbert, M.H. *Microstructure of Fine-Grained Sediments, from Mud to Shale*; Springer: New York, NY, USA, 1990.

21. Haese, R.R. The Biogeochemistry of Iron. In *Marine Geochemistry*; Schulz, H.D., Zabel, M., Eds.; Springer: Berlin/Heidelberg, Germany, 1998; Volume 7, pp. 241–270.

22. Raiswell, R.; Benning, L.G.; Davidson, L.; Tranter, M.; Tulaczyk, S. Schwertmannite in wet, acid, and oxic microenvironments beneath polar and polythermal glaciers. *Geology* **2009**, *37*, 431–434. [CrossRef]

23. Schwenzer, S.P.; Bridges, J.C.; McAdam, A.; Steer, E.D.; Conrad, P.G.; Kelley, S.P.; Wiens, R.C.; Mangold, N.; Grotzinger, J.; Eigenbrode, J.L.; et al. Modeling of sulphide microenvironments on Mars. In Proceedings of the 47th Lunar and Planetary Science Conference, Houston, TX, USA, 21–25 March 2016.

24. Steefel, C.I.; DePaolo, D.J.; Lichtner, P.C. Reactive transport modeling: An essential tool and a new research approach for the Earth sciences. *Earth Planet. Sci. Lett.* **2005**, *240*, 539–558. [CrossRef]

25. Kaszuba, J.P.; Yardley, B.W.D.; Andreani, M. Experimental Perspectives of Mineral Dissolution and Precipitation due to Carbon Dioxide-Water-Rock Interactions. *Rev. Mineral. Geochem.* **2013**, *77*, 153–188. [CrossRef]

26. Mu, N.; Schulz, H.-M.; Fu, Y.; Schovsbo, N.H.; Wirth, R.; Rhede, D.; van Berk, W. Berthierine formation in reservoir rocks from the Siri oilfield (Danish North Sea) as result of fluid-rock interactions: Part I. Characterization. *Mar. Petrol. Geol.* **2015**, *65*, 302–316. [CrossRef]

27. McMahon, S.; Anderson, R.P.; Saupe, E.E.; Briggs, D.E.G. Experimental evidence that clay inhibits bacterial decomposers: Implications for preservation of organic fossils. *Geology* **2016**, *44*, 867–870. [CrossRef]

28. Van Berk, W.; Fu, Y.; Schulz, H.-M. Creation of pre-oil-charging porosity by migration of source-rock-derived corrosive fluids through carbonate reservoirs: One-dimensional reactive mass transport modelling. *Petrol. Geosci.* **2015**, *21*, 35–42. [CrossRef]

29. Stawski, T.M.; Benning, L.G. Chapter Five—SAXS in Inorganic and Bioinspired Research. Research Methods in Biomineralization Science. In *Methods in Enzymology*; De Yoreo, J.J., Ed.; Elsevier: Amsterdam, The Netherlands, 2013; Volume 532, pp. 95–127.

30. Niederberger, M.; Pinna, N. Chapter 2: Aqueous and Nonaqueous Sol-Gel Chemistry. In *Metal Oxide Nanoparticles in Organic Solvents*; Niederberger, M., Pinna, N., Eds.; Springer: Berlin/Heidelberg, Germany, 2009; pp. 7–18.

31. Hoover, S.E.; Lehmann, D. The expansive effects of concentrated pyritic zones within the Devonian Marcellus Shale Formation of North America. *Q. J. Eng. Geol. Hydrogeol.* **2009**, *42*, 157–164. [CrossRef]

32. Aller, R.C. Quantifying solute distributions in the bioturbated zone of marine sediments by defining an average microenvironment. *Geochim. Cosmochim. Acta* **1965**, *44*, 1955–1965. [CrossRef]

33. Wirth, R. Focused Ion Beam (FIB) combined with SEM and TEM: Advanced analytical tools for studies of chemical composition, microstructure and crystal structure in geomaterials on a nanometre scale. *Chem. Geol.* **2009**, *261*, 217–229. [CrossRef]

34. Navrotsky, A. Energetic clues to pathways to biomineralization: Precursors, clusters, and nanoparticles. *Proc. Natl. Acad. Sci. USA* **2004**, *101*, 12096–12101. [CrossRef]

35. Ranade, M.R.; Navrotsky, A.; Zhang, H.Z.; Banfield, J.F.; Elder, S.H.; Zaban, A.; Borse, P.H.; Kulkarni, S.K.; Doran, G.S.; Whitfield, H.J. Energetics of nanocrystalline TiO_2 2002, Energetics of nanocrystalline TiO_2. *Proc. Natl. Acad. Sci. USA* **2002**, *99* (Suppl. 2), 6476–6481. [CrossRef]

36. Zhang, H.; Banfield, J.F. Thermodynamic analysis of phase stability of nanocrystalline titania. *J. Mater. Chem.* **1998**, *8*, 2073–2076. [CrossRef]

37. Hench, L.L.; West, J.K. The Sol-Gel Process. *Chem. Rev.* **1990**, *90*, 33–72. [CrossRef]

38. Chen, X.; Mao, S.S. Titanium Dioxide Nanomaterials: Synthesis, Properties, Modifications, and Applications. *Chem. Rev.* **2007**, *107*, 2891–2959. [CrossRef] [PubMed]

39. Niederberger, M. Nonaqueous Sol–Gel Routes to Metal Oxide Nanoparticles. *Acc. Chem. Res.* **2007**, *40*, 793–800. [CrossRef] [PubMed]

40. Pottier, A.; Chané, C.; Tronc, E.; Mazerolles, L.; Jolivet, J.-P. Synthesis of brookite TiO2 nanoparticles by thermolysis of TiCl4 in strongly acidic aqueous media. *J. Mater. Chem.* **2001**, *11*, 1116–1121. [CrossRef]

41. Li, J.-G.; Ishigaki, T.; Sun, X. Anatase, Brookite, and Rutile Nanocrystals via Redox Reactions under Mild Hydrothermal Conditions? Phase-Selective Synthesis and Physicochemical Properties. *J. Phys. Chem. C* **2007**, *111*, 4969–4976. [CrossRef]

42. Bhave, R.C.; Lee, B.I. Experimental variables in the synthesis of brookite phase TiO_2 nanoparticles. *Mater. Sci. Eng. A* **2007**, *467*, 146–149. [CrossRef]

43. Domingos, R.F.; Tufenkji, N.; Wilkinson, K.J. Aggregation of Titanium Dioxide Nanoparticles: Role of a Fulvic Acid. *Environ. Sci. Technol.* **2009**, *43*, 1282–1286. [CrossRef] [PubMed]

44. Yang, K.; Lin, D.; Xing, B. Interactions of Humic Acid with Nanosized Inorganic Oxides. *Langmuir* **2009**, *25*, 3571–3576. [CrossRef] [PubMed]

45. Hada, R.; Kabra, S.; Katara, S.; Rani, A.; Devra, V.; Amriphale, S.S. Synthesis of Nanosized Titania by sol Gel Route. *Indian J. Appl. Res.* **2013**, *3*, 49–50. [CrossRef]

46. Riaz, S.; Naseem, S. Controlled Nanostructuring of TiO2 Nanoparticles—A Sol Gel Approach. *J. Sol-Gel Sci. Technol.* **2015**, *74*, 299–309. [CrossRef]

47. Karimipour, M. Comparison of Acidic and Polymeric Agents in Synthesis of TiO_2 Nanoparticles via a Modified Sol-Gel Method. *World J. Nano Sci. Eng.* **2013**, *3*, 87–92. [CrossRef]

48. Khitab, A.; Ahmad, S.; Munir, M.J.; Kazmi, S.M.S.; Arshad, T.; Khushnood, R.A. Synthesis and applications of nano titania particles: A review. *Rev. Adv. Mater. Sci.* **2018**, *53*, 90–105.

49. Isley, S.L.; Penn, L.R. Relative brookite and anatase content in sol-gel-synthesized titanium dioxide nanoparticles. *J. Phys. Chem. B* **2006**, *110*, 15134–15139. [CrossRef] [PubMed]

50. Isley, S.L.; Penn, L.R. Titanium Dioxide Nanoparticles: Effect of Sol−Gel pH on Phase Composition, Particle Size, and Particle Growth Mechanism. *J. Phys. Chem. C* **2008**, *112*, 4469–4474. [CrossRef]

51. Isley, S.L.; Anderson, E.R.; Penn, R.L. Influence of ionic strength on brookite content in sol-gel synthesized titania before and after hydrothermal aging. *ECS Trans.* **2006**, *3*, 37–46.

52. Isley, S.L.; Jordan, D.S.; Penn, L.R. Titanium dioxide nanoparticles: Impact of increasing ionic strength during synthesis, reflux, and hydrothermal aging. *Mater. Res. Bull.* **2009**, *44*, 119–125. [CrossRef]

53. French, R.A.; Jacobson, A.R.; Kim, B.; Isley, S.L.; Penn, R.L.; Baveye, P.C. Influence of ionic strength, pH, and cation valence on aggregation kinetics of titanium dioxide nanoparticles. *Environ. Sci. Technol.* **2009**, *43*, 1354–1359. [CrossRef]

54. Arning, E.T.; Gaucher, E.C.; van Berk, W.; Schulz, H.-M. Hydrogeochemical models locating sulfate-methane transition zone in marine sediments overlying black shales: A new tool to locate biogenic methane? *Marine and Petroleum Geology* **2015**, *59*, 563–574. [CrossRef]

55. Bräuer, K.; Kämpf, H.; Faber, E.; Koch, U.; Nitzsche, H.M.; Strauch, G. Seismically triggered microbial methane production relating to the Vogtland—NW Bohemia earthquake swarm period 2000, Central Europe. *Geochem. J.* **2005**, *39*, 441–450.